Doping efficiency and confinement of donors in embedded and free standing Si nanocrystals

A. J. Almeida,[1] H. Sugimoto,[2] M. Fujii,[2] M. S. Brandt,[3] M. Stutzmann,[3] and R. N. Pereira[1,3,*]

[1]*Department of Physics and I3N, University of Aveiro, Campus Universitário de Santiago, 3810-193 Aveiro, Portugal*

[2]*Department of Electrical and Electronic Engineering, Graduate School of Engineering, Kobe University, Rokkodai, Nada, Kobe 657-8501, Japan*

[3]*Walter Schottky Institut and Physik-Department, Technische Universität München, Am Coulombwall 4, 85748 Garching, Germany*

(Received 8 October 2015; revised manuscript received 20 January 2016; published 17 March 2016)

Doping semiconductor nanocrystals (NCs) is a promising way to tailor the optical and electronic behavior of these materials to enable their use in (opto)electronic applications. Yet the practical exploitation of doping requires an understanding of its efficiency, and dependence on external environment, and of the electronic localization of dopant states due to confinement effects. Here, we experimentally probe the efficiency of doping of Si NCs grown in amorphous SiO_2 by means of phase segregation method. We estimate a P doping efficiency of these Si NCs of about 30% and from this we infer that most P dopants are incorporated at substitutional sites of the NCs lattice and thus act as donors. We further show that the doping efficiency in Si NCs varies by several orders of magnitude depending on their external environment. Charge traps associated with air molecules adsorbed to the NCs surface give rise to a strong compensation of donors. We observe that this process can be reverted by desorbing the molecules from the NCs surface under vacuum. Moreover, we experimentally assess the confinement energy of isolated donors in Si NCs from the temperature dependence of their magnetic resonance. From this, we provide experimental evidence for the confinement-induced increase of ionization energy of dopants with decreasing NC size previously predicted with *ab initio* calculations of doped Si NCs.

DOI: 10.1103/PhysRevB.93.115425

I. INTRODUCTION

Semiconductor nanocrystals (NCs) are materials with a few nanometer in diameter that display a wealth of remarkable size-specific optoelectronic properties that are not present in their bulk counterpart [1,2]. For example, NCs have large surface-to-volume ratios, can show luminescence [3] and exhibit a tunable band gap [1] when reduced to nanometer dimensions. These properties make semiconductor NCs promising as technological materials. For example, semiconductor NCs are being explored for use in light-emitting diodes [4], as light-absorbing materials in photovoltaics [5], in thermoelectric power devices [6], and in printable electronics such as thin film transistors [7]. Such applications of semiconductor NCs require a precise control of their electronic, optical, and magnetic properties. Doping with impurities is a promising means of tailoring these properties and thus major research efforts have been directed towards this topic in recent years [8–14]. With regard to electronic doping, progress in the incorporation of impurities has already been reported for NCs of CdSe [8,15–18], ZnSe [19–21], PbSe [9,22], InP [23], InAs [10,24], Si [25–29], and SiGe [30–32]. Owing to the potential compatibility with conventional electronics and the environmental inertness and abundance of silicon, doped Si NCs are particularly promising for future applications. Both *n*- and *p*-type doping of Si NCs by incorporation of P and B impurities, respectively, has already been reported [25,27,28,33–37].

The technological exploitation of doped Si NCs requires an understanding of the electronic doping efficiency. Several studies have investigated the introduction of dopants in free standing Si NCs [28,38], produced by plasma synthesis methods, as well as in Si NCs embedded in an oxide matrix [37,39–42]. In free standing P-doped Si NCs of sizes between 3-nm and 30-nm studies using secondary-ion mass spectrometry (SIMS) and inductively coupled plasma atomic emission spectrometry (ICP-AES) showed that the amount of P dopants incorporated in the NCs is approximately equal to the amount of P atoms introduced in the plasma during NC growth [28,38]. It was also observed that exposing the NCs to air leads to the formation of an oxide layer at the NCs surface. After removal of this surface oxide layer using a hydrofluoric (HF) acid treatment, only 5%–20% of the P atoms remained in the Si NCs [28,38]. This provided evidence for the segregation of P dopants to the NCs surface region during growth [28,38]. Studies have also reported the incorporation of P dopants in Si NCs embedded in an oxide matrix, prepared by phase segregation methods [25,37,39–43]. Photoluminescence measurements of P-doped Si NCs embedded in SiO_2 estimated the ratio between the effective density of P dopants incorporated in the NCs $[P]_{eff}$ and the nominal concentration of P dopants $[P]_{nom}$, which corresponded to the concentration of P atoms introduced in the films used to produce the Si NCs embedded in SiO_2 [41]. The values of $[P]_{eff}$ were estimated from the quenching of the PL signal, associated with Si dangling bonds (Si-dbs) at the NCs surface, that was observed upon doping the NCs with P. These studies found that $[P]_{eff}/[P]_{nom}$ was about 60% for $[P]_{nom} = 3.3 \times 10^{19}$ cm^{-3} and that it decreased to about 20% as $[P]_{nom}$ was increased to 1.2×10^{20} cm^{-3} [41]. These observations were associated with the segregation of P dopants to the interface between the NCs and the surrounding matrix, which should become more significant as the P content increases. For $[P]_{nom}$ over 1.2×10^{20} cm^{-3}, it was observed that $[P]_{eff}/[P]_{nom}$ increases and reaches about 50% for $[P]_{nom} = 1.7 \times 10^{20}$ cm^{-3}. It was suggested that this increase resulted from the introduction at high $[P]_{nom}$ of additional PL quenching centers associated with clusters of P dopants at the NCs interface or to matrix

*rnpereira@ua.pt; pereira@wsi.tum.de

 ©2016 American Physical Society

defects rather than from an effective increase in the amount of P dopants incorporated in the NCs [41]. Further studies on P-doped Si NCs embedded in silicon oxynitride ($SiO_{0.93}N_{0.22}$) directly assessed $[P]_{eff}$ using three-dimensional atom probe tomography [42]. These studies reported values of $[P]_{eff} = 4 \times 10^{20}$ cm^{-3} and found that about 20% of the P dopants are incorporated into the Si NCs, thus yielding $[P]_{eff} = 0.2[P]_{nom}$. It was further shown that an amount of P atoms corresponding to 30% of $[P]_{nom}$ is located at the interface between the NCs and their surrounding matrix [42].

Studies have also suggested that P dopants can be introduced in Si NCs embedded in a SiO_2 matrix through diffusion of P atoms during thermal annealing at about 1000°C from a spatially separated dopant source, namely a phosphosilicate thin-film with a thickness up to 0.5 nm [44–47]. By combining SIMS and x-ray photoelectron spectroscopy measurements with computational modeling of the experimental data, it was concluded that the incorporation of P dopants into Si NCs is aided by the presence of the SiO_2 matrix surrounding the NCs, which provides a barrier of about 1 eV for the diffusion of P atoms out of the NCs [45,47]. Further, it was shown that P dopants can be introduced in the Si NCs embedded in SiO_2 at concentrations up to six times the solubility limit of P in bulk Si [47].

Experimental studies have also investigated the relation between the amount of P dopants effectively introduced in the NCs ($[P]_{eff}$) and the quantity of donor electrons provided by electrically active P dopants [38–40]. Magnetic resonance measurements of free standing P-doped Si NCs showed that donor electrons from substitutional P in the Si NCs may become trapped at defects that introduce mid gap states in the NCs' electronic structure [38]. It was further shown that Si-dbs are a major source of these trap states in Si NCs. These defects were shown to compensate P donors in Si NCs and lead to a reduction of the concentration of electrons $[e^-]$ provided by P donors by about one order of magnitude with respect to $[P]_{eff}$ for NCs with diameters larger than ~ 12 nm [38]. In P-doped Si NCs with 4 nm in size and embedded in a SiO_2 matrix, transient current analyzes found that the concentration of carriers $[e^-]$ provided by P dopants for electronic transport within the NCs conduction band was only about 0.12% of $[P]_{nom}$ [40]. This observation was suggested to result from the incorporation of most P dopants in the NCs as interstitial impurities rather than as substitutional donors [39,40]. Interstitial P dopants in Si NCs are expected to induce deep trap states which cannot donate electrons but provide efficient carrier recombination, based on density functional theory calculations [39].

The electronic properties of doped Si NCs are also deeply influenced by the confinement of the charge carriers wave functions within the volume of the NCs. Early works on P donors in Si NCs embedded in SiO_2 using electron paramagnetic resonance (EPR) spectroscopy reported that the hyperfine interaction between the spin of donor electrons and the nuclear spin of their P nucleus increases with decreasing NC size [25]. This observation was associated to quantum confinement of the P donors in a volume smaller than the Bohr radius in bulk Si [25], as predicted by computational simulations [48]. Studies further showed that confinement of donors in Si NCs can also result from a reduction in the dielectric screening of the Coulomb interaction between the donor electron and its P nucleus [49]. Further theoretical studies have predicted that the activation energy of donors in Si NCs is a decreasing function of the NCs size due to quantum confinement [50,51]. Consequently, it is expected to be more difficult to electrically activate donors in smaller NCs. Nonetheless, this predicted increase in the activation energy of dopants in Si NCs has so far remained unverified experimentally. Experimental evidence of an increasing ionization energy with decreasing NC size has been given for the case of Co^{2+} ions in ZnSe NCs using magnetic circular dichroism spectroscopy [52]. From experimental data and *ab initio* calculations, it was concluded that the Co^{2+}/Co^{3+} level is energetically pinned, which results in an increase of the impurity ionization energy with increasing quantum confinement [52].

Magnetic resonance techniques have been used also to study the spatial distribution of the wave function of shallow interstitial Li donors in ZnO NCs [53–55]. In these studies, the confinement of the Li donors in small ZnO NCs up to 4.5 nm in size was probed using electron nuclear double resonance (ENDOR) via a dependence of the splitting of the hyperfine signal associated to the interaction between the donor electrons ($S = 1/2$) and their Li nuclei ($I = 3/2$). It was observed that the hyperfine interaction between the donor electron and the Li nucleus increases when reducing the NC size and this effect was associated to the confinement of the Li donor in the ZnO NCs [53,54]. Further, it was observed that this size dependence cannot be described by the effective mass approximation in the quantum confinement regime, i.e., when the radius of the NCs is smaller than the Bohr radius [54]. Studies using EPR and ENDOR spectroscopy have also identified the presence of shallow donors associated to substitutional Al atoms in ZnO NCs with 5 nm in size [56] via probing the hyperfine interaction interaction of the donor electrons and their Al nuclei ($I = 5/2$). From quantitative analysis of the observed hyperfine constant for shallow Al donors, it was shown that that the Al donors in the NCs could be described by effective mass theory. Magnetic resonance studies have also investigated the effect of surface acceptors on the ionization of donor electrons [57]. In these studies, compensation of shallow Li donors in ZnO NCs by acceptors located at the NCs surface was observed. There, it was observed that the EPR signal associated to unpaired spins in the NCs is only observed under photoexcitation. This observation was associated to the presence of deep acceptors in the NCs, which capture thermally excited donor electrons.

In the present work, using EPR spectroscopy, we investigate the impact of dopant confinement and external environment on the doping efficiency of P-doped Si NCs. We show that the doping efficiency in P-doped Si NCs varies by several orders magnitude, depending on their external environment. We associate this strong compensation of donors to air molecules adsorbed on the NCs surface and show that it can be reversed by desorbing the molecules from the NCs surface under vacuum. Further, we assess the confinement energy of isolated donors in Si NCs from the temperature dependence of their hyperfine signal. From these data, we infer that the ionization energy of donors in Si NCs increases with respect to their bulk counterpart, as predicted by previous *ab initio* calculations [48,50,51,58].

II. EXPERIMENTAL DETAILS

P-doped Si NCs were prepared as previously reported [59]. Si-rich phosphosilicate glass (PSG) films were first prepared on thin stainless steel plates by cosputtering Si, SiO_2, and P_2O_5 [26,35,59,60]. The average concentration of P atoms in the PSG films is 0.4 at.%, which corresponds to $[P]_{nom} = 2 \times 10^{20}$ cm^{-3}. The films were then peeled from the plates and annealed in a N_2 gas atmosphere at 1150 °C for 30 min to grow Si NCs in the PSG films [60,61]. During the growth, P impurity atoms are incorporated into the Si NCs [26,35,59,60]. The as-grown P-doped Si NCs become embedded in a SiO_2 matrix (hereafter, these samples are labeled SiNCs-SiO_2). The films containing P-doped Si NCs were ground to obtain a powder. To isolate Si NCs from the SiO_2 matrix, some of the powder was reacted in hydrofluoric (HF) acid solution (46 wt.%) for 20 minutes. This process results in the preparation of a HF solution containing isolated Si NCs. These isolated Si NCs were separated from the HF by centrifugation (4000 rpm, 1 min) followed by removal of the HF and a Si NC precipitate was obtained. Methanol was then added to the solution vessel to redisperse the Si NCs. The centrifugation and redispersion of the NCs in methanol was repeated several times to remove all HF. To obtain a dry powder of etched NCs from the dispersion of NCs in methanol, we evaporated the solvent under a low pressure Ar atmosphere. These samples of P-doped Si NCs liberated from their embedding SiO_2 matrix and with a H-terminated surface are labeled as SiNCs-H. To investigate the crystallinity and size distribution of the P-doped Si NCs used in this study, we performed high-resolution transmission electron microscopy (HRTEM) of SiNCs-H using a JEOL JEM-2100F microscope. For HRTEM observation, the NCs are drop-cast onto a carbon-coated Cu mesh.

Each sample of P-doped Si NCs used for EPR measurements was prepared by filling a few milligrams of dry powder containing P-doped Si NCs into suprasil quartz tubes. The powder was inserted into the tubes in an Ar-filled glovebox. After that the tubes were sealed with epoxy glue to prevent exposure of the NCs to air during measurements. The measurements were performed with a Bruker ESP 300E continuous-wave X-band spectrometer in absorption mode with a microwave frequency of $\nu = 9.38$ GHz. To perform low-temperature EPR, we used an Oxford Instruments ESR900 continuous-flow liquid He cryostat. All the EPR spectra shown in this study are normalized by the mass of Si NCs in the sample. In the case of SiNCs-SiO_2 samples, the mass fraction of NCs was about 0.2. In the case of SiNCs-H samples, the mass of NCs corresponds to the total mass of the sample and thus the mass fraction of NCs is 1.

III. RESULTS AND DISCUSSION

Figures 1(a) and 1(b) show two HRTEM images of SiNCs-H. There, we can observe NCs with lattice fringes of 0.314 nm, which correspond to {111} planes of the diamond structure of Si. TEM observations of a large number of NCs reveal that almost all NCs are single crystal and that doping does not affect the crystallinity. Figure 1(c) shows the size distribution of the P-doped Si NCs used in this study, extracted from the analysis of the HRTEM images of 40 NCs in SiNCs-H. The NCs size distribution can be approximated to a Gaussian function with a mean diameter of 5 nm and a standard deviation of 1.2 nm.

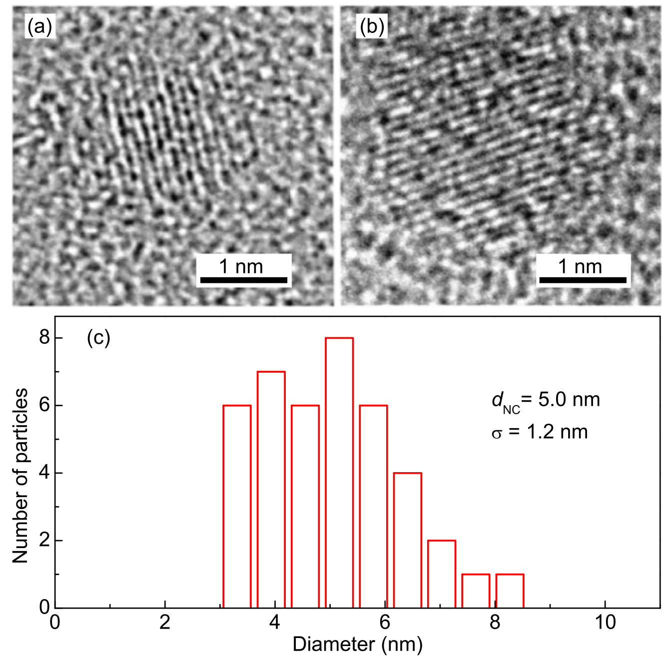

FIG. 1. (a) and (b) HRTEM images of SiNCs-H. The lattice fringes correspond to the {111} planes of Si. (c) NC size distribution extracted from the HRTEM images of SiNCs-H.

Curve (a) in Fig. 2 shows the EPR spectrum obtained for a SiNCs-SiO_2 sample. This spectrum can be well described by a computational simulation, shown in Fig. 3(a), that takes into account the spectral contributions of (i) a sharp signal located at $g = 2.002$ with a linewidth of 0.2. mT (green dash-dotted line), (ii) an asymmetric band with zero-crossing magnetic field at about 334 mT (blue line), (iii) a line at $g = 1.998$ (pink dashed line), and (iv) a pair of lines with median at $g = 1.998$ and separated by about 10.8 mT (purple dotted line). The line shape of (ii) results from the sum of two Lorentzian components and was obtained from the computational simulation of curve (c) of Fig. 2, which, as will be discussed below, only displays the EPR signal associated with Si-dbs. We assign (i) to EX centers in the oxide matrix surrounding the Si NCs [25,62,63], and the band (ii) to Si-dbs at the NCs surface [38]. Bands (iii) and (iv) are associated with the P donors in the Si NCs. Line (iii), which we label Exch, has a g value that is typical for P donor electrons in bulk Si and Si NCs [27,38,64,65]. This line has been attributed to exchange-coupled donor electrons [66]. Lines (iv), which we label hf(^{31}P), should result from the hyperfine interaction between the donor electrons spin $S = 1/2$ and the ^{31}P nucleus spin $I = 1/2$ [25]. In P-doped bulk crystalline Si, a hyperfine pair of lines with splitting of 4.2 mT and central g value at $g = 1.998$ is the characteristic fingerprint of substitutional, isolated P donors [64,67]. Thus the hf(^{31}P) signals observed in our NCs should be due to isolated donor electrons in the P-doped Si NCs. However, the splitting of 10.8 mT between the pair of hyperfine lines observed in our P-doped Si NCs is about 2.5 times larger than that observed in P-doped bulk crystalline Si. Studies of ZnO NCs doped with Li donors have also observed an enhancement of the hyperfine

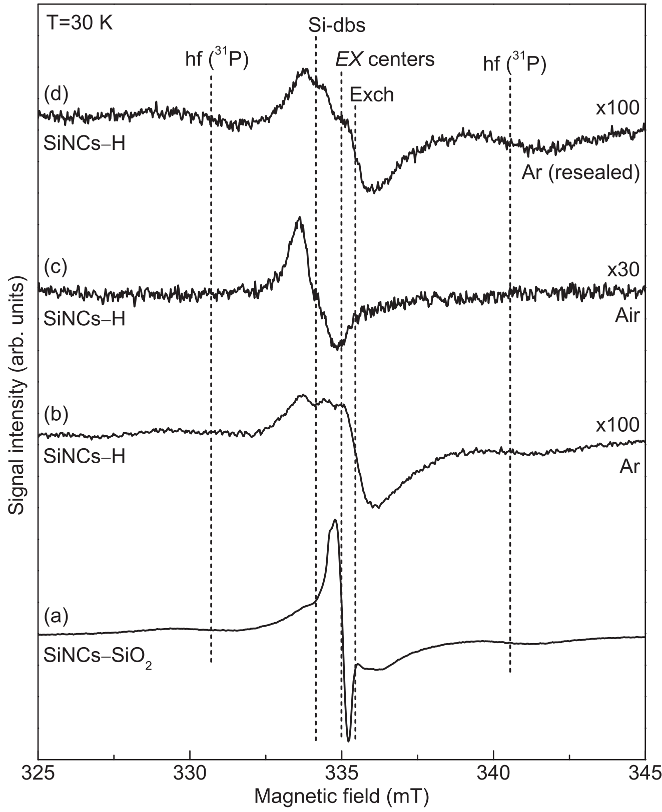

FIG. 2. EPR spectra of (a) SiNCs–SiO_2, (b) SiNCs–H sealed in an Ar atmosphere, (c) SiNCs–H exposed to air, and (d) SiNCs–H reasealed in an Ar atmosphere after exposure to air.

interaction between the donor electrons and the Li nuclei with respect to bulk ZnO [53,54]. In these studies, it was shown that this increase depends on the NC size and is caused by confinement of the Li donors in the NCs volume. Experimental studies showed that the magnitude of the hyperfine splitting can be used to infer the size of the P-doped Si NCs [25,49]. To verify if the hf(^{31}) signals observed in our P-doped Si NCs are compatible with the distribution of NC sizes obtained from the TEM images of our P-doped Si NCs (see Fig. 1), we simulated the expected hf(^{31}) signals taking into consideration the NCs size distribution and the size dependence of the hyperfine splitting in P-doped Si NCs. To this end, we used the convolution [49]

$$\int_0^\infty L_{d_{\mathrm{NC}},\sigma}(d)[F(B;\Gamma,B_-)+F(B;\Gamma,B_+)]dd, \quad (1)$$

where $L_{d_{\mathrm{NC}},\sigma}(d)$ is the size distribution of the NCs in the ensemble, which follows a Gaussian distribution with mean NC diameter d_{NC} and standard deviation $\sigma = 1.2$, d is NC diameter, and $F(B;\Gamma,B_\pm)$ are Lorentzian line shapes with center magnetic field positions $B_\pm = h\nu/g\mu_B \pm A_{\mathrm{NC}}(d)/2$ and width Γ. Here, h is the Planck constant, μ_B is the Bohr magneton, and $g = 1.998$. We use the value $\Gamma = 3$ mT and the NCs hyperfine splitting constant $A_{\mathrm{NC}}(d) = A_{\mathrm{bulk}} + (\rho/d_{\mathrm{NC}})^\tau$, with $A_{\mathrm{bulk}} = 4.16$ mT, $\rho = 16.3$ nm, and $\tau = 1.61$ [49]. Figure 3(c) shows the simulated hf(^{31}) signals for ensembles of P-doped Si NCs with $d_{\mathrm{NC}} = 3, 4, 5, 6, 8$, and 14 nm. Comparing the simulated hyperfine structures with those obtained

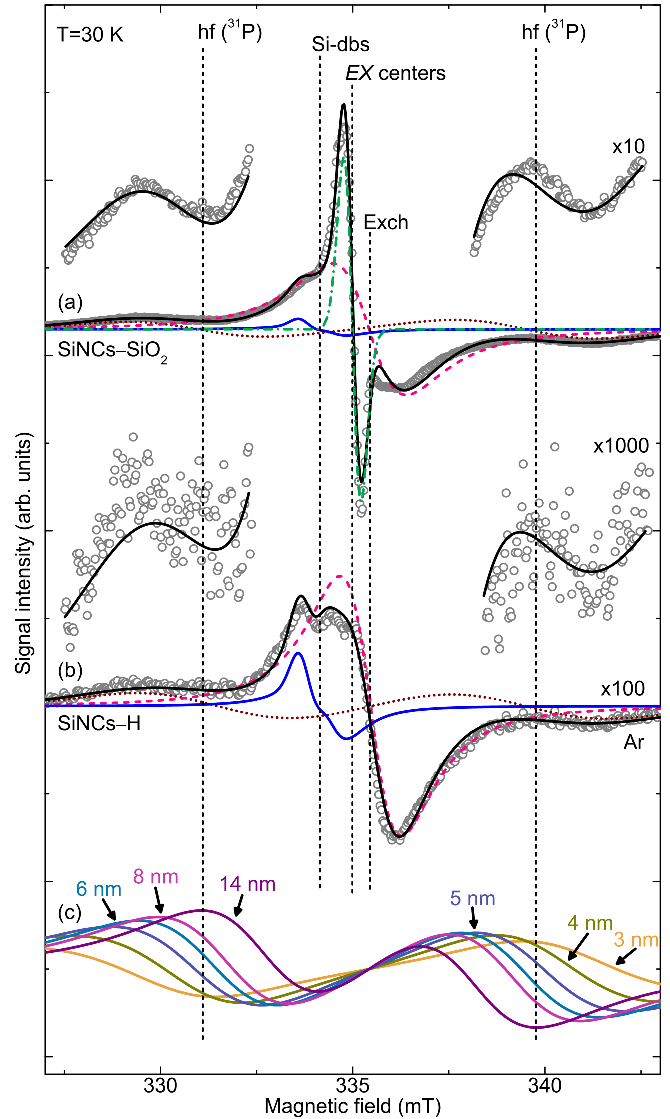

FIG. 3. EPR spectra of (a) SiNCs-SiO_2 and (b) SiNCs-H sealed in an Ar atmosphere. The spectra are shown together with their numerical fits. (c) Computational simulation of the hf(^{31}) signals for P-doped Si NCs with a gaussian size distribution with $\sigma = 1.2$ and $d_{\mathrm{NC}} = 3, 4, 5, 6, 8$, and 14 nm.

experimentally, we can see that the observed hyperfine signals agree with the distribution pattern of our Si NCs and a mean NC diameter of 5.5 ± 0.5 nm, which is compatible with the value of 5.0 nm obtained from the TEM images.

Curve (b) in Fig. 2 shows the EPR spectrum of a SiNCs-H sample, measured in an inert Ar atmosphere. From the computational simulation of this spectrum, shown in Fig. 3(b), we can see that the sharp signal at $g = 2.002$ due to EX centers disappears in relation to the EPR spectrum of SiNCs-SiO_2. This observation indicates that the etching procedure successfully removes the SiO_2 matrix surrounding the NCs. Further, in curve (b) of Fig. 3, we distinguish the signal due to Si-dbs at the NCs surface and the signals associated to P donors in the NCs, namely, the Exch signal due to exchange-coupled donor electrons and the pair of lines hf(^{31}P) due to isolated P donors in the Si NCs.

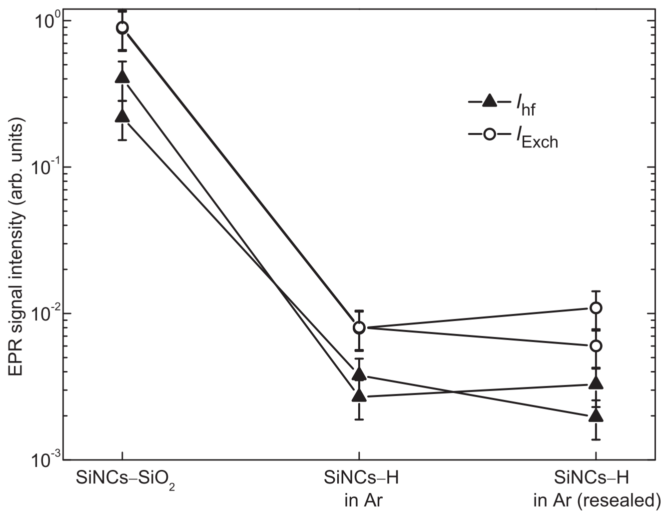

FIG. 4. EPR intensity of the hf(^{31}P) signal (black triangles) and of the Exch signal (black circles) observed in samples of P-doped Si NCs in different surrounding environments.

From the computational fits of the EPR spectra of P-doped Si NCs, we estimate the intensity of the EPR signals due to P donors in the Si NCs by numerical double integration of the corresponding resonance lines. The intensity of the hf(^{31}P) signal $I_{\rm hf}$ is given by the sum of the intensities of the two hf(^{31}P) lines, and the intensity of the Exch signal $I_{\rm Exch}$ is given by the intensity of the signal observed at $g = 1.998$. Figure 4 shows $I_{\rm Exch}$ (black circles) and $I_{\rm hf}$ (black triangle) for SiNCs-SiO$_2$ and SiNCs-H samples. There we see that the intensity of the signals due to P donors decreases by about two orders of magnitude upon removal of the oxide matrix surrounding the NCs. This observation indicates that the nature of the NCs surface has a strong effect on the doping efficiency of the Si NCs. A reason for this strong decrease may be the depassivation of Si-dbs at the NCs surface upon removal of the SiO$_2$ matrix surrounding the NCs. Such unpassivated Si-dbs may compensate P donors in the Si NCs and, thus, quench the EPR signals associated with donor electrons in the P-doped Si NCs. Another reason may be adsorption of residual H_2O and O_2 molecules to the NCs surface, which provide trap states for electrons donated by P donors in the Si NCs. The trends of $I_{\rm Exch}$, $I_{\rm hf}$, and $I_{\rm Exch}/I_{\rm hf}$ displayed in Fig. 4 are identical for two sets of samples, which shows the reproducibility of the data.

To further investigate the effect of the nature of the environment surrounding the NCs on the P-doping efficiency of Si NCs, we exposed SiNCs-H samples to air by unsealing the sample tubes and measuring the EPR spectrum of the NCs during exposure to air. This is shown in curve (c) of Fig. 2 for one sample. We can see that the signals due to P donors in the Si NCs disappear upon exposure of the NCs to air and that the EPR spectrum now only displays the signal at $g = 2.006$ due to Si-dbs. This observation indicates that exposure of the NCs to air leads to the compensation of all the P donors incorporated in the Si NCs. After exposure to air, we left the samples in a vacuum chamber for 20 minutes and then resealed the sample tubes under Ar atmosphere. The EPR spectrum measured after resealing the P-doped Si NCs is shown as curve (d) in Fig. 2. There, we see that the hf(^{31}P) and the Exch signals attributed to P donors in the Si NCs reappear. In Fig. 4, we can also see that the EPR signals due to P donors in the sample SiNCs-H have a similar intensity before exposure to air and after exposure to air followed by resealing in a Ar atmosphere. This indicates that the observed compensation of P donors in the Si NCs by exposure to air is a reversible process, which may be related to the transfer of donor electrons to air molecules that adsorb to the NCs surface upon their exposure to air. Leaving the NCs in vacuum leads to the desorption of air molecules from the NCs surface and consequent elimination of the trap states that lead to the compensation of P donors.

Previous studies showed that the adsorption of air molecules can alter the electrical properties of amorphous Si due to surface charge transfer [68,69]. Recent studies also reported that the electrical conductivity measured in air of films of H-terminated Si NCs doped with P is about one order of magnitude higher than that of films of undoped H-terminated Si NCs [70]. However, it was further observed that the conductivity of films of P-doped Si NCs decreases over time and after about four hours of exposure of the films to air the conductivity is about the same as that of undoped Si NCs. Our present results indicate that this effect may in part be caused by the transfer of donor electrons to air molecules that adsorb to the NCs surface upon their exposure to air, which leads to the compensation of donor electrons and makes the P-doped Si NCs effectively undoped. Studies on Li-doped ZnO NCs capped with a $Zn(OH)_2$ layer using EPR spectroscopy have also reported a compensation effect, where the electrons provided by Li donors become trapped in deep surface acceptors [57]. It was further observed that this process could be reverted by photo-excitation, which transfers the electrons from the acceptors to the donors and makes both sites paramagnetic [57].

We have studied the dependence of the EPR intensity of the hf(^{31}P) signal observed for the P-doped Si NCs on temperature T. Figure 5(a) shows the temperature dependence of $I_{\rm hf}$ measured for a SiNCs−SiO$_2$ sample (blue dots). There we can see that the intensity of the hf(^{31}P) signal scales as T^{-1} between 15 and 120 K, confirming that this EPR signal displays a Curie behavior within this temperature range. This observation enables us to infer that the density of electrons donated by isolated P in the NCs remains constant within this temperature range [38]. Thus there is no thermal excitation of P donors up to 120 K. From this, we can infer a lower limit for the ionization energy of isolated P donors from their bound ground state to conduction band (CB) states. At 0 K, we have a certain density $n^0_{\rm d,0}$ of donor electrons bound to their isolated P nuclei. As T increases, the donor electrons may be thermally excited to CB states and electrons populate CB states with a density n, which is given by [71]

$$n^2 = \frac{N_{\rm c}}{2}\left(n^0_{\rm d,0} - n\right)e^{-E_{\rm d}/k_{\rm B}T}, \qquad (2)$$

where $N_{\rm c} = (2\pi m^*_{\rm Si} k_{\rm B} T/h^2)^{3/2}$ is the effective density of CB states, $m^*_{\rm Si} = 3[1/0.92(m_0) + 2/(0.19 m_0)]^{-1}$ is the electron effective mass and m_0 is the free-electron mass, and $k_{\rm B}$ is the Boltzmann constant. The maximum density of electrons in the CB is $n^0_{\rm d,0}$, i.e., when all neutral P are thermally excited. Figure 5(b) shows $P_+ = n/n^0_{\rm d,0}$, which corresponds to the

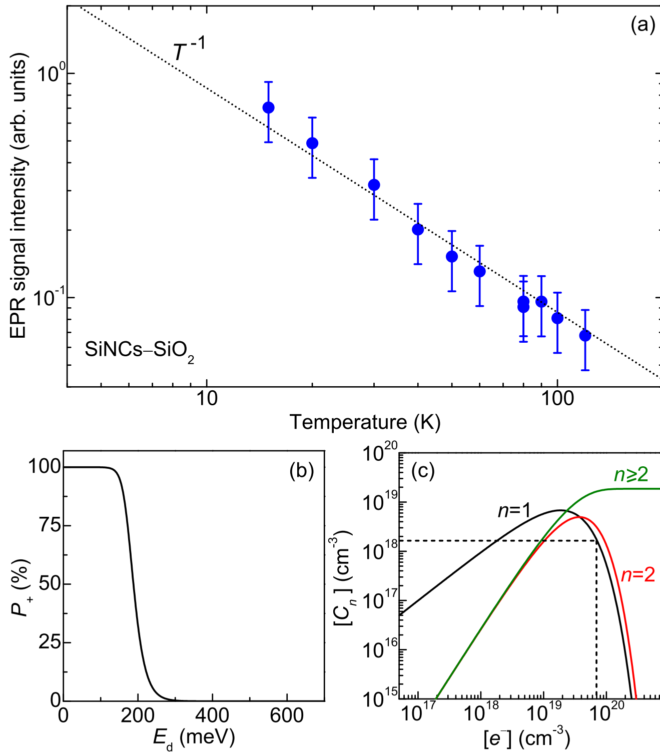

FIG. 5. (a) Temperature dependence of the EPR signal intensity of the pair of hf(^{31}P) signals in SiNCs−SiO$_2$. (b) Dependence of the fraction of thermally excited P donors P_+ as a function of the excitation energy $E_{\rm d}$ at a temperature of 120 K. (c) Ensemble density of donor clusters with n donor electrons $[C_n]$ with $n = 1$, $n = 2$, and $n > 2$ as a function of the donor electron density $[e^-]$. This calculation was performed for a NC ensemble with a Gaussian size distribution with average NC size equal to 5.0 nm and $\sigma = 1.2$.

fraction of P donors that are thermally excited for different values of $E_{\rm d}$ and calculated for $T = 120$ K. In this figure, we see that the onset of P_+ occurs for $E_{\rm d} \approx 240$ meV. From this, we infer that the excitation energy of isolated P donors in P-doped Si NCs is at least 240 meV. This value of $E_{\rm d}$ is significantly higher than that required to ionize a donor electron in bulk crystalline Si (45.6 meV) [72]. Previous theoretical works have predicted that the ionization energy of a single P dopant in a H-terminated Si NC of 4 nm should be about 200 meV due to an increase in the confinement of P donors in the NCs with respect to the bulk [50]. More recent studies using density functional theory calculations predicted that a P donor in a Si NC with 1.5 nm in size and with its surface terminated with OH provides a donor state with an ionization energy of 510 meV [39]. Here, using temperature-dependent EPR spectroscopy, we estimate a minimum value of about 240 meV for the ionization energy of P dopants in Si NCs with a mean diameter of 5 nm, which is considerably larger than the ionization energy for P dopants in bulk Si. An increase in the dopant ionization energy with respect to that in the bulk counterpart has also been observed in P-doped Si nanowires [73]. There, it was observed that the conductivity of the nanowires decreases with decreasing wire radius. It was further possible to estimate the dopant ionization energy in the P-doped Si nanowires from the analysis of their experimental data using a model for the size-dependent dopant ionization energy based on the dielectric mismatch between the nanowire and its surroundings [73].

We have also estimated the density of isolated donors in our P-doped Si NCs by comparing the intensity of the hf(^{31}P) signal (see Fig. 4) with that of a known spin standard consisting of a P-doped bulk crystalline Si. From this analysis, we obtain a density of isolated donors of 1.6×10^{18} cm^{-3} in SiNCs-SiO$_2$ and of about 1.1×10^{16} cm^{-3} in SiNCs-H measured in Ar atmosphere. From the density of isolated donor electrons, we can estimate the total amount of donor electrons in our P-doped Si NCs using a statistical analysis. Accordingly, the probability p_n that a donor electron is located in a NC with n donor electrons may be given by

$$p_n(n,d_{\rm NC},x) = \sum_d L_{d_{\rm NC}},\sigma(d) \frac{n\, W_x^{N(d)}(n)}{\sum_{j=1}^{\infty} j\, W_x^{N(d)}(j)}, \qquad (3)$$

where $[e^-]$ is the total density of donor electrons in the NCs ensemble, $W_x^{N(d)}(n)$ is the binomial distribution, with $N(d) = \pi n_{\rm Si} d^3/6$ (number of lattice sites in the NC) and $x = [e^-]/n_{\rm Si}$. Here, $n_{\rm Si} = 5 \times 10^{22}$ cm^{-3} is the atomic density of bulk crystalline Si. Further, $L_{d_{\rm NC},\sigma}(d)$ is the size distribution of the NCs in the ensemble, which follows a Gaussian distribution with a mean NC diameter $d_{\rm NC} = 5$ nm and standard deviation $\sigma = 1.2$ nm as described above. From Eq. (3), we can calculate the ensemble density of donor clusters with n donor electrons $[C_n] = [e^-] \times p_n/n$. Figure 5(c) shows $[C_n]$ as a function of $[e^-]$ for $n = 1$, $n = 2$, and $n \geqslant 2$. From the data shown in this figure, we can see that the density of isolated donor electrons $[C_1]$ that we obtain from EPR corresponds to two possibilities of $[e^-]$. However, only for the highest value of $[e^-]$ the amount of exchange-coupled donors in the NCs is higher than that of isolated donors and can result in an Exch signal that is more intense than the hf(^{31}P) signal, as we observe in our EPR measurements (see Fig. 4). Thus, from the analysis of Fig. 5, we estimate a value of $[e^-] \approx 6 \times 10^{19}$ cm^{-3} in SiNCs-SiO$_2$.

Comparing the values of $[e^-] \approx 6 \times 10^{19}$ cm^{-3} and of $[{\rm P}]_{\rm nom} = 2 \times 10^{20}$ cm^{-3} obtained for SiNCs−SiO$_2$, we infer that the electronic doping efficiency $[e^-]/[{\rm P}]_{\rm nom}$ is about 30% for these NCs. This result contrasts with previously reported studies of P-doped Si NCs embedded in SiO$_2$, which estimated that the ratio between (substitutional) P donors providing electrons to the NCs CB and $[{\rm P}]_{\rm nom}$ was only 0.12% [40]. This low value for the P doping efficiency of Si NCs was proposed to result from the incorporation of P in interstitial sites of the NCs [40]. However, our current study demonstrates that a sizable amount of P donor atoms are incorporated at substitution sites. If we consider the incorporation efficiencies of P dopants in Si NCs embedded in SiO$_2$ given in Ref. [41], i.e., 20%–60%, we can assume that in our NCs we have $[{\rm P}]_{\rm eff} = (0.4 \pm 0.2)\,[{\rm P}]_{\rm nom}$. We estimate $[e^-] = 0.3\,[{\rm P}]_{\rm nom}$, which means that $[e^-]$ is very close to $[{\rm P}]_{\rm eff}$. This indicates that nearly all P dopants provide a donor electron, which occurs if P dopants are introduced in the NCs as substitutional impurities. We note that in Ref. [40] the amount of electrons provided by P donors in the NCs was determined by transient current analysis via measuring the voltage-dependent ionized carrier density. This method only detects the fraction of donor electrons that are excited to

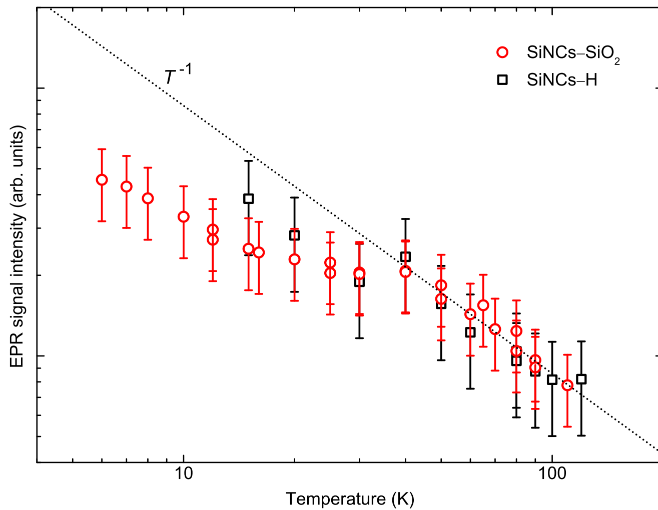

FIG. 6. Temperature dependence of the EPR signal intensity of Exch signals in SiNCs−SiO_2 (black squares) and SiNCs−H (red circles).

the NCs CB and participate in the current through the NCs network. In contrast, our method detects the amount donor electrons bound to their P atoms. We should also note at this point that in a very recent work [47], it has been proposed that P atoms may indeed be introduced in Si NCs prepared by phase segregation methods at concentrations higher than the solubility limit of P in bulk Si.

In the SiNCs-H sample measured in Ar, the P doping efficiency decreases drastically to about 0.3%, as can be seen from the decrease by two orders of magnitude of the corresponding value of I_{hf} with respect to that measured for the SiNCs-SiO_2 sample, see Fig. 4. Such low electronic doping efficiency is in par with that previously reported for free standing P-doped Si NCs [38]. A reason for the low doping efficiency observed in the SiNCs-H sample may be an enhancement of charge trap states at the NCs surface upon removal of the NCs surrounding SiO_2 matrix by HF etching. These trap states may result from residual H_2O and O_2 molecules adsorbed at the NCs surface.

We now discuss briefly the temperature dependence of the Exch signals observed in the P-doped Si NCs. Figure 6 shows this dependence for SiNCs-SiO_2 (black squares) and for SiNCs-H (red circles). There, we can see that the intensity of the Exch signal follows a Curie behavior for temperatures down to 40 K. Below 40 K, the intensity of the Exch signal strongly deviates from the Curie behavior. In a previous EPR study, we have similarly observed a deviation of the intensity of the signal of exchange coupled donor electrons from Curie behavior with decreasing temperature [66]. In the studied P-doped Si NCs, the signal from exchange coupled donor electrons originated mostly from donor dimers [66], i.e., from Si NCs with only two donor electrons (donor clusters with $n = 2$), for which the electronic structure and corresponding temperature dependence can be relatively easily calculated [74]. The deviation from the Curie behavior has been explained based on the freezing of the donor dimers into their singlet electronic state ($S = 0$, EPR silent) with decreasing temperature [66,74]. In the case of the P-doped Si NCs studied in the present work, we expect that the signal due to exchange coupled donor electrons results from donor clusters with n larger than 2, taking into account the relatively large donor electron concentration estimated ($[e^-] \approx 6 \times 10^{19}$ cm^{-3}). As can be seen from Fig. 5(c), for this value of $[e^-]$ the density of donor clusters with $n > 2$ is much larger than the density of donor dimers ($n = 2$). Therefore the EPR signal from exchange coupled donor electrons has significant contributions from donor clusters with a wide range of n values, i.e., $n = 2$, 3, 4 and so on, for which the electronic structure and its temperature dependence becomes virtually impossible to predict. However, we expect that the ground state of donor clusters with even number of electrons ($n = 2$, 4, 6,. . .) has zero electron spin and, therefore, these donor clusters become EPR invisible with decreasing temperature, which is qualitatively compatible with the temperature dependence shown in Fig. 6.

IV. CONCLUSIONS

In summary, we have used EPR spectroscopy to study P doping of Si NCs formed in amorphous SiO_2 by means of phase segregation method. From our quantitative EPR data, we estimate the density electrons donated by P atoms incorporated in substitutional sites of the Si NCs. Comparison of this electron density with the density of P atoms introduced during the synthesis of the Si NCs enabled us to infer that the efficiency of n-type doping of these Si NCs with P impurities during grown is in the range of 30%. Moreover, we observe that the donor electron density decreases by about two orders of magnitude when the NCs are removed from their native SiO_2 matrix and exposed to air. We interpret this observation as charge compensation of P donors in the NCs by traps associated to air molecules adsorbed to the NCs surface. We further show that this process can be reverted by desorbing the molecules from the NCs surface under vacuum. Furthermore, from the temperature dependence of the EPR signal associated with isolated P donors in the Si NCs, we assess the ionization energy of isolated P donors in Si NCs with a mean diameter of 5 nm to be > 240 meV. From this, we provide experimental evidence for the predictions made with *ab initio* calculations of doped Si NCs, according to which confinement induces an increase in the ionization energy of dopants with decreasing NC size.

ACKNOWLEDGMENTS

The authors acknowledge the financial support from Fundação para a Ciência e a Tecnologia (FCT) via projects PTDC/FIS/112885/2009 and RECI/FIS-NAN/0183/2012 (FCOMP-01-0124-FEDER-027494) and from Fundação Calouste Gulbenkian via *Prémio de Estímulo à Investigação*. A.J.A. thanks FCT for a PhD Grant (SFRH/BD/79223/2011). This work has been partially developed in the scope of the project I3N (UID/CTM/50025/2013), financed by national funds through the Fundação para a Ciência e a Tecnologia/Ministério da Educação e Ciências (FCT/MEC) and when applicable cofinanced by FEDER under the PT2020 Partnership Agreement.

[1] A. D. Yoffe, Adv. Phys. **51**, 799 (2002).
[2] S. D. Bader, Rev. Mod. Phys. **78**, 1 (2006).
[3] A. P. Alivisatos, Science **271**, 933 (1996).
[4] M. G. Panthani and B. A. Korgel, Ann. Rev. Chem. Biomol. Eng. **3**, 287 (2012).
[5] H. W. Hillhouse and M. C. Beard, Curr. Opin. Colloid Interface Sci. **14**, 245 (2009).
[6] R. Y. Wang, J. P. Feser, J.-S. Lee, D. V. Talapin, R. Segalman, and A. Majumdar, Nano Lett. **8**, 2283 (2008).
[7] D. L. Klein, R. Roth, A. K. L. Lim, A. P. Alivisatos, and P. L. McEuen, Nature (London) **389**, 699 (1997).
[8] A. Sahu, M. S. Kang, A. Kompch, C. Notthoff, A. W. Wills, D. Deng, M. Winterer, C. D. Frisbie, and D. J. Norris, Nano Lett. **12**, 2587 (2012).
[9] M. S. Kang, A. Sahu, C. D. Frisbie, and D. J. Norris, Adv. Mater. **25**, 725 (2013).
[10] D. Mocatta, G. Cohen, J. Schattner, O. Millo, E. Rabani, and U. Banin, Science **332**, 77 (2011).
[11] C. Wang, B. L. Wehrenberg, C. Y. Woo, and P. Guoyt-Sionnest, J. Phys. Chem. B **108**, 9027 (2004).
[12] N. Pradhan, D. Goorskey, J. Thessing, and X. G. Peng, J. Am. Chem. Soc. **127**, 17586 (2005).
[13] N. Pradhan and D. D. Sarma, J. Phys. Chem. Lett. **2**, 2818 (2011).
[14] V. A. Vlaskin, N. Janssen, J. van Rjssel, R. Beaulac, and D. R. Gamelin, Nano Lett. **10**, 3670 (2010).
[15] C. Tuinenga, J. Jasinski, T. Iwamoto, and V. Chikan, ACS Nano **2**, 1411 (2008).
[16] S. Roy, C. Tuinenga, F. Fungura, P. Dagtepe, and V. C. J. Jasinski, J. Phys. Chem. C **113**, 13008 (2009).
[17] A. W. Wills, M. S. Kang, K. M. Wentz, S. E. Hayes, A. Sahu, W. L. Gladfelter, and D. J. Norris, J. Mater. Chem. **22**, 6335 (2012).
[18] D. K. Kim, A. T. Fafarman, B. T. Dirrol, S. H. Chan, T. R. Gordon, C. B. Murray, and C. R. Kagan, ACS Nano **7**, 8760 (2013).
[19] D. J. Norris, N. Yao, F. T. Charnock, and T. A. Kennedy, Nano Lett. **1**, 3 (2001).
[20] N. Pradhan and X. Peng, J. Am. Chem. Soc. **129**, 3339 (2007).
[21] N. Pradhan, D. M. Battaglia, Y. Liu, and X. Peng, Nano Lett. **7**, 312 (2007).
[22] S. J. Oh, N. E. Berry, J.-H. Choi, E. A. Gaulding, T. Paik, S.-H. Hong, C. B. Murray, and C. R. Kagan, ACS Nano **7**, 2413 (2013).
[23] R. Xie and X. Peng, J. Am. Chem. Soc. **131**, 10645 (2009).
[24] S. M. Geyer, P. M. Allen, L.-Y. Chang, C. R. Wong, T. P. Osedach, N. Zhao, V. Bulovic, and M. G. Bawendi, ACS Nano **4**, 7373 (2010).
[25] M. Fujii, A. Mimura, S. Hayashi, Y. Yamamoto, and K. Murakami, Phys. Rev. Lett. **89**, 206805 (2002).
[26] M. Fujii, Y. Yamaguchi, Y. Takase, K. Ninomiya, and S. Hayashi, Appl. Phys. Lett. **87**, 211919 (2005).
[27] A. R. Stegner, R. N. Pereira, K. Klein, R. Lechner, R. Dietmueller, M. S. Brandt, M. Stutzmann, and H. Wiggers, Phys. Rev. Lett. **100**, 026803 (2008).
[28] X. D. Pi, R. Gresback, R. W. Liptak, S. A. Campbell, and U. Kortshagen, Appl. Phys. Lett. **92**, 123102 (2008).
[29] Y. Nakamine, N. Inaba, T. Kodera, K. Uchida, R. N. Pereira, A. R. Stegner, M. S. Brandt, M. Stutzmann, and S. Oda, Jpn. J. Appl. Phys., Part 1 **50**, 025002 (2011).
[30] B. Stoib, T. Langmann, S. Matich, T. Antesberger, N. Stein, S. Angst, N. Petermann, R. Schmechel, G. Schierning, D. E. Wolf, H. Wiggers, M. Stutzmann, and M. S. Brandt, Appl. Phys. Lett. **100**, 231907 (2012).
[31] B. Stoib, A. Greppmair, N. Petermann, H. Wiggers, M. Stutzmann, and M. S. Brandt, Adv. Electron. Mater. **2015**, 1400029 (2015).
[32] D. J. Rowe and U. R. Kortshagen, APL Mater. **2**, 022104 (2014).
[33] R. Lechner, A. R. Stegner, R. N. Pereira, R. Dietmueller, M. S. Brandt, A. Ebbers, M. Trocha, H. Wiggers, and M. Stutzmann, J. Appl. Phys. **104**, 053701 (2008).
[34] R. Lechner, H. Wiggers, A. Ebbers, J. Steiger, M. S. Brandt, and M. Stutzmann, Phys. Status Solidi RRL **1**, 262 (2007).
[35] M. Fujii, Y. Yamaguchi, Y. Takase, K. Ninomiya, and S. Hayashi, Appl. Phys. Lett. **85**, 1158 (2004).
[36] R. K. Baldwin, J. Zou, K. A. Pettigrew, G. J. Yeagle, R. D. Britt, and S. M. Kauzalarich, Chem. Commun. (Cambridge), No. 6, 658 (2006).
[37] K. Sumida, K. Ninomiya, M. Fujii, K. Fujio, S. Hayashi, M. Kodama, and H. Ohta, J. Appl. Phys. **101**, 033504 (2007).
[38] A. R. Stegner, R. N. Pereira, R. Lechner, K. Klein, H. Wiggers, M. Stutzmann, and M. S. Brandt, Phys. Rev. B **80**, 165326 (2009).
[39] D. König, S. Gutsch, H. Gnaser, M. Wahl, M. Kopnarski, J. Göttlicher, R. Steininger, M. Zacharias, and D. Hiller, Sci. Rep. **5**, 09702 (2015).
[40] S. Gutsch, J. Laube, D. Hiller, W. Bock, M. Wahl, M. Kopnarski, H. Gnaser, B. Puthen-Veettil, and M. Zacharias, Appl. Phys. Lett. **106**, 113103 (2015).
[41] S. Gutsch, A. M. Hartel, D. Hiller, N. Zakharov, P. Werner, and M. Zacharias, Appl. Phys. Lett. **100**, 233115 (2012).
[42] H. Gnaser, S. Gutsch, M. Wahl, R. Schiller, M. Kopnarski, D. Hiller, and M. Zacharias, J. Appl. Phys. **115**, 034304 (2014).
[43] A. Mimura, M. Fujii, S. Hayashi, D. Kovalev, and F. Koch, Phys. Rev. B **62**, 12625 (2000).
[44] M. Perego, C. Bonafos, and M. Fanciulli, Nanotech. **21**, 025602 (2010).
[45] M. Perego, G. Seguini, and M. Fanciulli, Surf. Interface Anal. **45**, 386 (2013).
[46] M. Mastromatteo, E. Arduca, E. Napolitani, G. Nicotra, D. D. Salvador, L. Bacci, J. Frascaroli, G. Seguini, M. Scuderi, G. Impellizzeri, C. Spinella, M. Perego, and A. Carnera, Surf. Interface Anal. **46**, 393 (2014).
[47] M. Perego, G. Seguini, E. Arduca, J. Frascaroli, D. D. Salvador, M. Mastromatteo, A. Carnera, G. Nicotra, M. Scuderi, C. Spinella, G. Impellizzeri, C. Lenardi, and E. Napolitani, Nanoscale **7**, 14469 (2015).
[48] D. V. Melnikov and J. R. Chelikowsky, Phys. Rev. Lett. **92**, 046802 (2004).
[49] R. N. Pereira, A. R. Stegner, T. Andlauer, K. Klein, H. Wiggers, M. S. Brandt, and M. Stutzmann, Phys. Rev. B **79**, 161304(R) (2009).
[50] G. Cantele, E. Degoli, E. Luppi, R. Magri, D. Ninno, G. Iadonisi, and S. Ossicini, Phys. Rev. B **72**, 113303 (2005).
[51] T. L. Chan, M. L. Tiago, E. Kaxiras, and J. R. Chelikowsky, Nano Lett. **8**, 596 (2008).
[52] N. S. Norberg, G. M. Dalpian, J. R. Chelikowsky, and D. R. Gamelin, Nano Lett. **6**, 2887 (2006).

[53] S. B. Orlinskii, J. Schmidt, P. G. Baranov, D. M. Hofmann, C. de Mello Donegá, and A. Meijerink, Phys. Rev. Lett. **92**, 047603 (2004).
[54] S. B. Orlinskii, J. Schmidt, E. J. J. Groenen, P. G. Baranov, C. de Mello Donegá, and A. Meijerink, Phys. Rev. Lett. **94**, 097602 (2005).
[55] S. B. Orlinskii, H. Blok, E. J. J. Groenen, J. Schmidt, P. G. Baranov, C. M. Donegá, and A. Meijerink, Magn. Reson. Chem. **43**, S140 (2005).
[56] S. B. Orlinskii, J. Schmidt, P. G. Baranov, V. Lorrmann, I. Riedel, D. Rauh, and V. Dyakonov, Phys. Rev. B **77**, 115334 (2008).
[57] S. B. Orlinskii, H. Blok, J. Schmidt, P. G. Baranov, C. de Mello Donegá, and A. Meijerink, Phys. Rev. B **74**, 045204 (2006).
[58] G. M. Dalpian and J. R. Chelikowsky, Phys. Rev. Lett. **96**, 226802 (2006).
[59] M. Fukuda, M. Fujii, H. Sugimoto, K. Imakita, and S. Hayashi, Opt. Lett. **36**, 4026 (2011).
[60] M. Fujii, K. Toshikiyo, Y. Takase, Y. Yamaguchi, and S. Hayashi, J. Appl. Phys. **94**, 1990 (2003).
[61] H. Sugimoto, M. Fujii, Y. Yamaguchi, M. Fukuda, K. Imakita, and S. Hayashi, J. Appl. Phys. **110**, 063528 (2011).
[62] K. Fujio, M. Fujii, K. Sumida, S. Hayashi, M. Fujisawa, and H. Ohta, Appl. Phys. Lett. **93**, 021920 (2008).
[63] M. Fujii, A. Mimura, S. Hayashi, K. Yamamoto, C. Urakawa, and H. Ohta, J. Appl. Phys. **87**, 1855 (2000).
[64] P. R. Cullis and J. R. Marko, Phys. Rev. B **11**, 4184 (1975).
[65] P. R. Cullis and J. R. Marko, Phys. Rev. B **1**, 632 (1970).
[66] R. N. Pereira, A. J. Almeida, A. R. Stegner, M. S. Brandt, and H. Wiggers, Phys. Rev. Lett. **108**, 126806 (2012).
[67] G. Feher, Phys. Rev. **114**, 1219 (1959).
[68] M. Tanielian, Philos. Mag. B **45**, 435 (1982).
[69] C. G. B. Garret and W. H. Brattain, Phys. Rev. **78**, 3801 (1955).
[70] R. N. Pereira, S. Niesar, W. B. You, A. F. da Cunha, N. Erhard, A. R. Stegner, H. Wiggers, M.-G. Willinger, M. Stutzmann, and M. S. Brandt, J. Phys. Chem. C **115**, 20120 (2011).
[71] H. Sapoval and C. Hermann, *Physics of Semiconductors*, 1st ed. (Springer-Verlag, New York, 1995).
[72] A. K. Ramdas and S. Rodriguez, Rep. Prog. Phys. **44**, 1297 (1981).
[73] M. T. Björk, H. Schmid, J. Knoch, H. Riel, and W. Riess, Nat. Nanotech. **4**, 103 (2009).
[74] A. J. Almeida, R. N. Pereira, and M. S. Brandt, Appl. Phys. Lett. **101**, 093108 (2012).